Journal of Molecular Catalysis A: Chemical 342–343 (2011) 74–82

Contents lists available at ScienceDirect

Journal of Molecular Catalysis A: Chemical

journal homepage: www.elsevier.com/locate/molcata

Synthesis and antioxidant activity of phosphorylated polysaccharide from *Portulaca oleracea* L. with $H_3PW_{12}O_{40}$ immobilized on polyamine functionalized polystyrene bead as catalyst

Tong Chen [a], Ling Zhu [a], Xiaoyan Liu [a], Yuanyuan Li [a], Chuande Zhao [a], Zhigang Xu [a], Wenfu Yan [b], Haixia Zhang [a,*]

[a] Key Laboratory of Nonferrous Metal Chemistry and Resources Utilization of Gansu Province, Lanzhou University, Lanzhou 730000, China
[b] State Key Laboratory of Inorganic Synthesis Preparative Chemistry, College of Chemistry, Jilin University, Changchun 130012, China

ARTICLE INFO

Article history:
Received 4 March 2011
Received in revised form 19 April 2011
Accepted 20 April 2011
Available online 28 April 2011

Keywords:
Esterifications
Polysaccharide
Catalyst
Antioxidant activity

ABSTRACT

Esterification of polysaccharide had been carried out by catalysis using a series of catalysts, which were synthesized by $H_3PW_{12}O_{40}$ (HPW) immobilized on chloromethylated polystyrene bead (PSC) and named as PS-EDA-HPW, PS-DETA-HPW, PS-TETA-HPW and PS-(AST-HPW)$_n$ according to different linker in the reaction system. The catalysts were characterized by FTIR spectroscopy, nitrogen adsorption, X-ray diffraction and inductively coupled plasma atomic emission spectrophotometer. PS-(AST-HPW)$_n$ showed the highest efficacy on esterification of polysaccharide. Four phosphorylated derivatives (POP1-p) of a native polysaccharide (POP1) from *Portulaca oleracea* L. with different degree of substitution (DS_p) were obtained using PS-(AST-HPW)$_n$ as the catalyst. Chemical equilibrium was established as quickly as 10 h with the content of P more than 5%. Compared with native POP1, POP1-p exhibited superior antioxidant activities *in vitro*, which indicated that phosphorylated modification could enhance antioxidant activities of POP1. It was obvious that the DS_p had a significant effect on the antioxidant activity.

1. Introduction

Oxidation is essential biological process to many organisms for the production of energy [1]. However, reactive oxygen species (ROS) generated in this process can cause damage to a wide range of essential bio-molecules, such as DNA, and they have been associated with carcinogenesis, coronary heart disease and many other health problems related to advancing age [2–4]. Antioxidants are the substances used for restraining oxidation of cellular oxidizable substrates. They exert their effects by scavenging ROS, activating a battery of detoxifying proteins, or preventing the generation of ROS [5]. Thus, it is essential to develop and utilize effective antioxidants which can protect the human body from free radicals and retard the progress of many chronic diseases [6]. At present, many antioxidants are used for industrial processing. For example, they are widely used in food industry as food thickener and stabilizer [7].

In recent years, studies have shown that polysaccharide displays excellent radical scavenging activity against superoxide radical and hydroxyl radical. Antioxidant activities of polysaccharide depend on their structural parameters, including glycosidic bond of the main chain, sugar unit, flexibility and configuration of the chains and glycosidic branching [8]. To increase antioxidant activities, molecular modification and structure improvement of polysaccharide become a hot topic. Recently, chemical modifications of polysaccharide by esterification, oxidation and hydroxypropylation have been used to prepare custom-made derivatives with desirable functionality attributes [9,10]. Most studies have demonstrated that antioxidant activities of polysaccharide are greatly increased by molecular modification [11–13]. For example, the phosphorylation of polysaccharide could not only enhance the water solubility but also change the chain conformation, resulting in alteration of their antioxidant activities [11,14].

Portulaca oleracea L. is a green annual herb of Portulacaceae family, and was known as “Long-lived grass” in China [15,16]. Polysaccharide obtained from *Portulaca oleracea* L. (POP) was the main effective ingredient with many weak biological activities, such as enhancing immunity, anti-oxidation, and anti-cancer [17]. In the present study, we extracted POP and synthesized four phosphorylated polysaccharides, and hoped that phosphorylated modification could improve the biological activities of POP.

The phosphorylation modification of polysaccharide was an esterification process essentially, which was very difficult to accomplish due to the complicated structures of polysaccharide

* Corresponding author. Tel.: +86 931 8912510; fax: +86 931 8912582.
E-mail addresses: zhanghx@lzu.edu.cn, chentong2010007@163.com (H. Zhang).

1381-1169/$ – see front matter © 2011 Elsevier B.V. All rights reserved.
doi:10.1016/j.molcata.2011.04.014

[14]. Conventional homogenous catalysts widely used for esterification include H_2SO_4, HCl, HF and $ClSO_2OH$ [18,19]. However, they had some disadvantages, such as their corrosive nature, the existence of side reactions and the fact that the catalyst could not be easily separated from the reaction mixture [20]. Furthermore, polysaccharide in strongly acidic conditions would be depolymerized severely due to the long reaction time, which led to loss original biological activities of polysaccharides. In order to solve these problems, use of a solid acid catalyst that could be recovered and reused easily was proposed [21–23]. Different heterogeneous catalysts such as zeolites, mixed metal oxide, sulfated zirconia, niobic acid and carbohydrate acid derivatives supported heteropoly acids (HPAs) had been studied in the esterification reaction [24–26]. However, the majority of them had narrow pore size distributions, and macromolecules like POP could not be in and out catalysts freely. Chloromethylated polystyrene bead (PSC) with a macroreticular structure could provide large pore size distributions and was suitable to be in and out for macromolecules.

HPAs were widely used in numerous acid-catalysed reactions due to their strong Brönsted acidity [27]. A number of porous supports had been used for supporting HPAs [28–30]. However, due to the high solubility of HPAs in polar solvent, HPAs physically adsorbed on the surface of the support could be easily leached out [31]. Chemical bonding had been carried out to immobilize HPAs on some materials. To increase immobilization of various HPAs, the acid molecules were attached via spacers. Immobilization reduced leaching of HPAs into the reaction system, even of polar nature, to a minimum. $H_3PW_{12}O_{40}$ (HPW) was the most stable substance among all HPAs and had received increasing attention due to their simple preparation and high acidity [32]. To the best of our knowledge, investigation of HPW immobilized on PSC as a catalyst for the esterification reaction process of macromolecules had not been reported, such as the phosphorylated modification of polysaccharide.

In the present work, we prepared a series of solid acid catalysts with HPW immobilized on PSC (PSC_{HPW}). PSC_{HPW} was characterized by FT-IR spectra, nitrogen adsorption, X-ray diffraction (XRD). The activity and stability of PSC_{HPW} were tested by the phosphorylated modification of POP as a model reaction. Phosphorylated POP was studied including DS_p, weight-average molecular mass (Mw) and chain conformation, and antioxidant activities *in vitro*. The effects of chain conformation and phosphate groups on the antioxidant activities of POP were discussed.

2. Materials and methods

2.1. Materials and reagents

P. oleracea L. was collected from the mountain area in Weinan city, Shaanxi Province, China. The crude POP from *P. oleracea* L. was obtained from Shaanxi Lixin biotechnology Co., Ltd.

Mesoporous SBA-15 silica molecular sieves (SBA-15) were obtained from Jilin University High-Tech. Co. Ltd (Jilin, China). 3-Aminopropyl-trimethoxysilane (APES) and 4-aminostyrene (AST) were purchased from Alfa Aesar (New Jersey, USA). PSC was purchased from Xian Xiaolan Technology Co., Ltd (Shaanxi, China). HPW, triethylamine, tetrabutyl ammonium bromide (TBAB), azobis-isobutyronitrile (AIBN) and hydroquinone were from Tianjin Guangfu Chemical Research Institute (Tianjin, China). Ethylenediamine (EDA), diethylenetriamine (DETA) and triethylene tetramine (TETA) were purchased from Sinopharm Chemical Reagent Co. Ltd (Shanghai, China).

Papain was from Beijing Huamei Biotechnology Co., Ltd (China). SephadexG-100 was from Pharmacia Co. (Sweden). 3-Phosphonopropionic acid was purchased from Alfa Aesar(Shanghai, China). Crocus, hydrogen peroxide (H_2O_2), 1,1-diphenyl-2-picrylhydrazyl (DPPH), ferrozine, ferric chloride, trichloroacetic acid (TCA), and potassium ferricyanide were purchased from Sinopharm Chemical Reagent Co. Ltd (Shanghai, China). Ethylenediaminetetraacetic acid (EDTA) disodium salt, Nitro blue tetrazolium (NBT), phenazine methosulfate (PMS), nicotinamide adenine dinucleotide-reduced (NADH) and butylated hydroxyanisole (BHA) were purchased from Tianjin Damao Chemical Research institute (Tianjin, China). Ascorbic acid (V_C) was purchased from Sigma (St. Louis, MO, USA).

2.2. Synthesis of PSC_{HPW}

2.2.1. Synthesis of PS-EDA, PS-DETA and PS-TETA

Two grams of PSC was swelled in 20 mL of ethanol for 2 h, and the solution was added to a 100 mL three-necked glass flask fitted with a reflux condenser and magnetic stirrer. Sodium hydroxide (0.5 g) and the phase transfer catalyst TBAB (0.1 g) dissolved in 20 mL of water were added to the reaction system. Finally, 25 mL of EDA, DETA or TETA was dropped into the three-necked glass flask quickly. The reaction mixture was heated in an oil-bath at 80 °C with continuous stirring for 6 h. The polymer beads were filtered and rinsed thoroughly with distilled water and ethanol to remove the residual impurities. The products were left to dry completely in vacuum for 12 h for the obtainment of PS-EDA, PS-DETA and PS-TETA.

2.2.2. Synthesis of PS-AST

Two grams of PSC was swelled by Section 2.2.1 processes. Triethylamine (5 mL), TBAB (0.1 g) and hydroquinone (5 mg) dissolved in 10 mL ethanol was added in the reaction system. Finally, AST (0.8 g) dissolved in 20 mL of ethanol was dropped into the reaction system quickly. The reaction mixture was heated under a N_2 atmosphere in an oil-bath 80 °C with continuous stirring for 6 h. The polymer beads were filtered, rinsed and dried by Section 2.2.1 processes. PS-AST was obtained.

2.2.3. Polymerization [33]

PS-AST (2.0 g) and AST (2.0 g) were added to 30 mL of ethanol, and the polymerization was performed by the initiating of AIBN (1.0 wt.% of monomer) under N_2 atmosphere at 70–80 °C for 24 h. The final product was filtered, intensively washed with acetone and ethanol respectively, and then dried under vacuum at 60 °C overnight. PS-$(AST)_n$ was obtained.

2.2.4. Immobilization of HPW

HPW (2.0 g) dissolved in 20 mL of ethanol was added to the flask, and the solution was added slowly to each support with appropriate quantity. The reaction mixture was then heated in an oil-bath at 80 °C with continuous stirring for 12 h. The polymer beads were filtered, rinsed and dried by the process described in Section 2.2.1. The materials were denoted as PS-EDA-HPW, PS-DETA-HPW, PS-TETA-HPW and PS-$(AST\text{-}HPW)_n$.

The routes for synthesis of catalysts were showed in Fig. 1.

2.2.5. Immobilization of HPW on SBA-15

Immobilization of HPW on SBA-15 was prepared according to the method of Liu and Ding with some modifications [34]. Two grams of dried SBA-15 and APES (2.5 mL) were added into freshly distilled toluene refluxing for 48 h. The obtained solid material was immersed in ethanol of HPW (2.0 g dissolved in 20 mL of ethanol) with stirring at 80 °C for 12 h. The solid was then dried in vacuum to obtain HPW anchored mesoporous catalyst, denoted as SBA-15-NH_2-HPW.

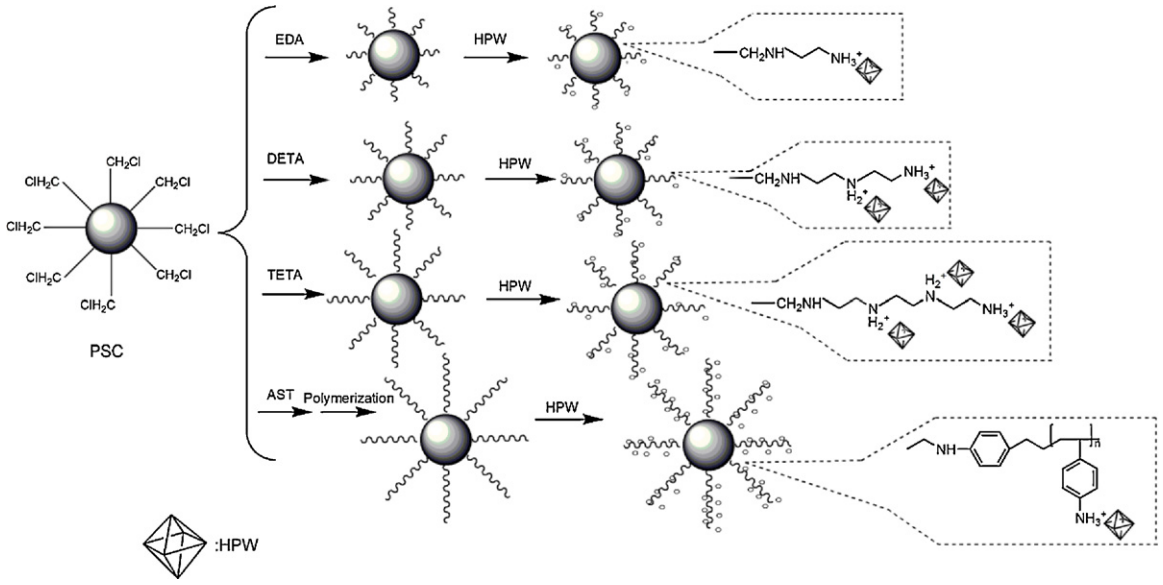

Fig. 1. Preparation procedures of catalysts.

2.3. Characterization

2.3.1. Characterization of catalysts

The IR spectra were recorded on a FLS920 FT-IR spectrophotometer (Edinburgh, England).

Nitrogen adsorption–desorption isotherms were measured with a Tristar 3000 Surface Area and Porosimetry analyzer (Micromeritics Instrument Corp., USA). Brunauer–Emmett–Teller (BET) surface area, S_{BET}, was determined from the linearity of BET equation. Pore size and its distribution were calculated using desorption isotherm branch and the Barrett–Joyner–Halenda (BJH) formula.

The XRD patterns from 3.0° to 80° were recorded with a D/max-2400 (Rigaku, Japan) using Cu Kα radiation.

The P and W contents of the catalysts were determined on an inductively coupled plasma atomic emission spectrophotometer (ICP-AES) IRIS ER/S (TJA Company, USA).

The water absorption capacity of catalysts was determined by weighing the water retained. The amount of water adsorption was measured by immersing the sample in water, at room temperature for 24 h. Then, the samples were taken out, wiped with tissue paper and weighed. The water adsorption amount (m) was calculated using the following formula:

$$m = m_1 - m_0$$

where m_1 is the mass of swollen sample and m_0 is the initial mass.

2.3.2. Characterization of the phosphorylated polysaccharide

Mw of the phosphorylated polysaccharide was determined by high-performance gel-filtration chromatography (HPGFC) on a Waters 2695 instrument equipped with three WATO columns, and a Waters 2414 Refractive Index Detector (RID). 1 mg/mL sample solution was injected in each run using 0.05 mol/L Na_2SO_4 as the mobile phase. The analysis was performed at 25 °C with a flow rate of 0.7 mL/min. The HPGFC system was calibrated with T-series Dextran standards (T-5, T-25, T-50, T-150 and T-270).

The P content of the phosphorylated polysaccharide was determined with ICP-AES, and DS_p which represented the average number of phosphate groups on each monosaccharide residue, was calculate using the following formula:

$$DS_p = \frac{162 \times P\%}{3100 - 84 \times P\%}$$

^{13}C NMR spectra of 40 mg/mL solution in D_2O were recorded on a Bruker Avance 600 MHz spectrometer (Germany) at 40 °C with 2,2-dimethyl-2-silapentane-5-sulfonate (DSS) as internal standard.

2.4. Catalytic experiment

The crude POP (10 g) was purified according to the reported method [35,36]. After purification, three kinds of purified POP (named as POP1, POP2 and POP3) were obtained, and their purities were up to 94%. Their yields were 42.3%, 4.5%, 6.2%, respectively. POP1 was used for further experiment, and the molecular mass of POP1 was 55.8 kDa.

POP1 (0.2 g) was suspended in anhydrous DMF (20 mL) at room temperature with stirring for 30 min. Then 3-phosphonopropionic acid (1.0 g) and catalyst (0.2 g) were added and the mixture was stirred at 40 °C. The reaction was stopped at different time, and the mixture was cooled to room temperature. The catalyst was filtered, rinsed and dried. The filtrate was dissolved in water, and was dialyzed (molecular weight cutoff 8–14 kDa) by distilled water for 24 h to remove DMF and potential degradation products. Phosphorylated polysaccharide (POP1-p) was obtained after lyophilizing.

2.5. Assay for antioxidant activities

2.5.1. Hydroxyl radical-scavenging activity

The hydroxyl radical scavenging activity of polysaccharide was measured according to the method of Zhang [9]. Samples were dissolved in distilled water at the concentration of 0.1–5 mg/mL. The sample solution (1.0 mL) was incubated with 2 mmol/L EDTA–Fe^{2+} (0.5 mL), 3% H_2O_2 (1.0 mL) and 0.36 mg/mL crocus (1.0 mL) in 1.0 mL of sodium phosphate buffer (PBS, 150 mM, pH 7.4) for 30 min at 37 °C. Hydroxyl radical was detected by monitoring absorbance at 520 nm. V_C was used as positive control. The hydroxyl radical scavenging effect was calculated using the following formula:

$$\text{Scavenging effect}\,(\%) = \left[\frac{A_1 - A_0}{A_2 - A_0}\right] \times 100\%$$

where A_0 was the absorbance of sample substituted with distilled water, A_1 was the absorbance of the sample mixed with reaction solution, A_2 was the absorbance of sample substituted with distilled water and H_2O_2 substituted with PBS.

2.5.2. Superoxide anion scavenging activity

The superoxide radical scavenging ability of polysaccharide was assessed by the method of Nishimiki et al. [37]. In this experiment, superoxide anion radicals were generated in 4.5 mL of Tris–HCl buffer solution (16 mM, pH 8.0) containing 0.5 mL of NBT (74 μM) solution, 0.5 mL of NADH (397 μM) solution and varying concentrations of samples (0.1–5.0 mg/mL). The reaction was started by adding 0.5 mL of PMS (45 μM) solution to the mixture. The reaction mixture was incubated at room temperature for 5 min and the absorbance was read at 560 nm by a spectrophotometer against blank samples. The decreased absorbance of the reaction mixture indicated that the scavenging activity of the corresponding polysaccharide to superoxide radical increased. V_C was used as positive control. The scavenging capability of polysaccharide to superoxide radical was calculated using the following equation:

$$\text{Scavenging effect}\,(\%) = \left(1 - \frac{A_1}{A_0}\right) \times 100\%$$

where A_0 was the absorbance of mixture solution without sample; A_1 was the absorbance of the sample mixed with reaction solution.

2.5.3. DPPH radical scavenging assay

The ability of polysaccharide on scavenging DPPH radical was measured according to the method of Shimada with some modifications [38]. Briefly, a 0.2 mmol/L solution of DPPH in 50% methanol was incubated with different concentrations of the samples (0.1–5.0 mg/mL). The reaction mixture was shaken well and incubated for 20 min at room temperature and the absorbance of the resulting solution was read at 517 nm against a blank. BHA was used as positive control. The radical scavenging activity was measured as a decrease in the absorbance of DPPH and was calculated using the following equation:

$$\text{Scavenging effect}\,(\%) = \left(1 - \frac{A_1}{A_0}\right) \times 100\%$$

where A_0 was the absorbance of DPPH solution without sample; A_1 was the absorbance of the sample mixed with DPPH solution.

2.5.4. Metal chelating assay

The ferrous ion-chelating ability of polysaccharide was investigated with a slightly modified method of Braca et al. [39]. Samples in different concentrations (0.2–5 mg/mL) were mixed with $FeCl_2$ (0.1 mL, 2 mM) and ferrozine (0.4 mL, 5 mM), shaken well, and kept still for 10 min at room temperature. Then the absorbance of the mixture was determined at 562 nm. EDTA was used as positive control. The ferrous ion-chelating activity was given by the following equation:

$$\text{Chelating ability}\,(\%) = \left(1 - \frac{A_1}{A_0}\right) \times 100\%$$

where A_0 was the absorbance of mixture solution without sample; A_1 was the absorbance of the sample mixed with reaction solution.

2.5.5. Reducing power assay

The reducing power of polysaccharide was determined referring to the reference with some modifications [40]. Different concentrations of samples (0.1–5.0 mg/mL, 2.5 mL) were mixed with 2.5 mL of PBS (150 mM, pH 6.6) and 2.5 mL of potassium ferricyanide (1%). The mixture was incubated at 50 °C for 20 min. Then TCA (10%, w/v) was added to the mixture. Finally, the solution was mixed with distilled water and $FeCl_3$ (0.1%, w/v), the absorbance was measured at 700 nm against a blank. A higher absorbance indicated a higher reducing power. BHA was used as positive control.

3. Results and discussion

3.1. Structural characterization of catalysts

3.1.1. FT-IR spectra

The primary structures of catalysts were identified by comparing their FTIR absorption bands to those of SBA-15, PSC and bulk HPW (Fig. 2). The Keggin structure of bulk HPW was identified by four characteristic absorption bands appearing at 1079 cm^{-1} (stretching frequency of P–O in the central PO_4 tetrahedron), 981 cm^{-1} (terminal bands for W=O in the exterior), 892 cm^{-1} (stretching vibration of W–O_b–W bridges between corner sharing octahedras) and 798 cm^{-1} (stretching vibrations of W–Oc–W bridges between edge sharing octahedras) [41]. Compared with FTIR spectra of PSC, four catalysts showed some characteristic IR bands (the Keggin-type polyanion fingerprint) of HPW at 1079 cm^{-1}, 981 cm^{-1} and 892 cm^{-1}. The FT-IR data implied the retention of Keggin structure during the immobilization of HPW on PSC. The two strong peaks at 826 cm^{-1} and 671 cm^{-1} might be assigned to the stretching vibration of C–Cl bond, which had disappeared in all of PSC_{HPW}. The IR spectral results suggested that the synthesis of PSC_{HPW} was successful and efficacious.

Compared with FTIR spectra of SBA-15, SBA-15-NH_2-HPW also showed characteristic bands of HPW, although somewhat different from those of bulk HPW: both the P–O band (1079 cm^{-1}) was buried in the strong and broad Si–O–Si band and Si–O band of SBA-15. W=O band and W–O_b–W vibration in SBA-15-NH_2-HPW showed the prominent bands at 977 cm^{-1} and 889 cm^{-1}, and appeared the blue-shift compared with absorption of HPW at 981 cm^{-1} and 892 cm^{-1}.

3.1.2. Acid capacity and hydrophilic characters of PSC_{HPW}

The acid capacity of PSC_{HPW} was an important parameter to speed up the esterification. It was observed that catalyst acidity increased significantly with increasing loading of amine groups on catalyst. In other words, the amount of HPW introduced was also increased (Table 1). The content of amine groups was different on four PSC_{HPW} due to different substrate in the reaction system. The sequence of the content of amine groups was PS-EDA-HPW < PS-DETA-HPW < PS-TETA-HPW < PS-$(AST\text{-}HPW)_n$. As a result, PS-$(AST\text{-}HPW)_n$ showed the strongest acid capacity with 19.49% W content and 0.291% P content.

The absorption behaviors of PSC_{HPW} in water were investigated in Table 1. The saturated adsorption of water on the four catalysts was in the sequence PS-EDA-HPW < PS-DETA-HPW < PS-TETA-HPW < PS-$(AST\text{-}HPW)_n$. This uptake of water was likely related to the interaction of the highly polar H_2O molecules with the amine groups very well in the catalysts. The result clearly showed that water formed in the esterification could be removed from the medium and adsorbed by the catalysts, which speed the reaction to get dynamic equilibrium within 10 h.

3.1.3. Physical adsorption of N_2

The characterizations of pore properties of PSC before and after the modification were obtained by N_2 adsorption study in the isotherms (Fig. 3). It was reported that they exhibited a typical type II isotherms in the IUPAC classifications with a H3 type hysteresis loop appearing, which were characteristic by the presence of a large proportion of mesopores and macropores [42]. The same type of isotherms indicated that the structure of PSC remained constant and unchanged after modification.

Parameters of surface areas and pore sizes of catalysts were given in Table 1. The bulk Keggin HPW had a negligible S_{BET}

Table 1
Catalytic activity and physical properties of catalysts.

Catalyst	Acid capacities			WA[d] (mg/g)	S_{BET}[e] (m^2/g)	D_{pore}[f] (nm)
	W[a] (wt.%)	P[b] (wt.%)	HPW[c] (wt.%)			
PS-EDA-HPW	4.26	0.073	5.56%	427	35	21.71
PS-DETA-HPW	5.33	0.079	6.93%	469	34	20.31
PS-TETA-HPW	5.81	0.088	7.55%	487	28	19.33
PS-(AST-HPW)$_n$	19.49	0.291	25.34%	553	18	17.31
PSC	–	–		380	36	22.37
SBA-15-NH_2-HPW	3.57	0.059	4.64%	331	395	5.87
SBA-15	–	–		306	524	7.20

[a] W, the W content of catalyst.
[b] P, the P content of catalyst.
[c] HPW, the percent of HPW loading on each support.
[d] WA, water absorption.
[e] S_{BET}, surface area.
[f] D_{pore}, pore size.

(<0.2 m^2/g), while PSC had 36 m^2/g. The smaller S_{BET} of PSC_{HPW} (35, 34, 28 and 18 m^2/g, respectively), were a consequence of modification. However, the S_{BET} of SBA-15 and SBA-15-NH_2-HPW were 524 m^2/g and 395 m^2/g, which were much larger than PSC_{HPW}. The pore sizes of PSC_{HPW} ranged from 21.71 to 17.31 nm, which were much larger than those of SBA-15 and SBA-15-NH_2-HPW.

3.1.4. XRD

Bulk HPW had a cubic structure and was characterized by the corresponding reflections in the XRD patterns (Fig. 4). PSC exhibited a non-crystalline to amorphous form. No reflections of HPW were detected due to the low content of HPW on PS-EDA-HPW, which showed that HPW was highly dispersed on the support. The catalysts (PS-DETA-HPW, PS-TETA-HPW and PS-(AST-HPW)$_n$) showed some new diffraction peaks at 2θ regions of 6–8° and 26–28° due to the loading of HPW. It was observed that the cubic structure of HPW was formed on the surface of catalysts. HPW was randomly immobilized on the surface or in the pores of the catalysts. These structural properties of PSC_{HPW} promoted the catalytic activity.

3.1.5. Esterification reaction

The performances of the catalysts for the esterification between POP1 and 3-phosphonopropionic acid were shown in Fig. 5. Without catalyst, the reaction progressed slowly and approached chemical equilibrium with the content of P in POP1-p less than 1.00%. The reaction sped up slightly with SBA-15-NH_2-HPW as the catalyst and the content of P approached to 1.73%. Compared with SBA-15-NH_2-HPW, PSC_{HPW} catalyzed the reaction much more rapidly. Especially, chemical equilibrium was established more quickly for 10 h with the content of P more than 5% using PS-(AST-HPW)$_n$. It was observed that acid strength of the catalysts was an important parameter to the speed of the esterification. The S_{BET} of SBA-15-NH_2-HPW was larger than that of PSC_{HPW}, but the pore size of the later was much longer than that of the former. According to the results, macromolecule (POP1) may diffuse freely as it went into the pores of PSC_{HPW}, which permitted the equilibrium to shift towards the product side. It was well known that SBA-15 is a unique material and had the well-order mesoporous structure and the large surface area. However, the pore size of SBA-15-NH_2-HPW was

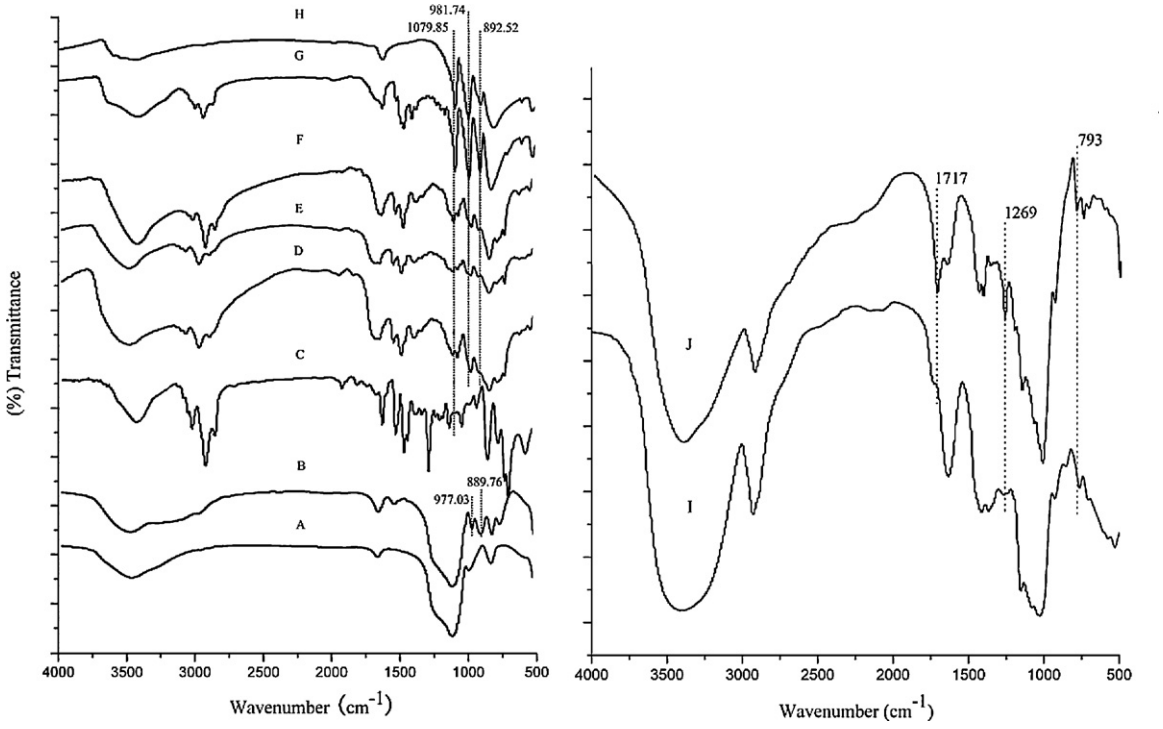

Fig. 2. FT-IR spectra of SBA-15 (A), SBA-15-NH_2-HPW (B), PSC (C), PS-EDA-HPW (D), PS-DETA-HPW (E), PS-TETA-HPW (F), PS-(AST-HPW)$_n$ (G), HPW (H), POP1(I), POP1-p4 (J).

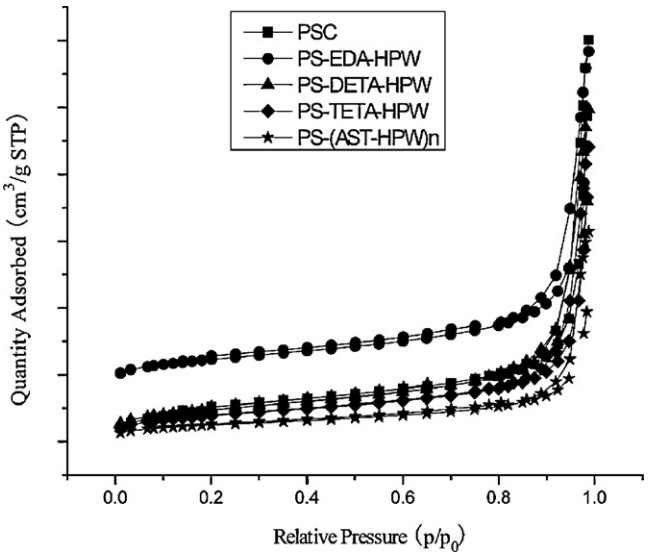

Fig. 3. Adsorption isotherms of the catalysts.

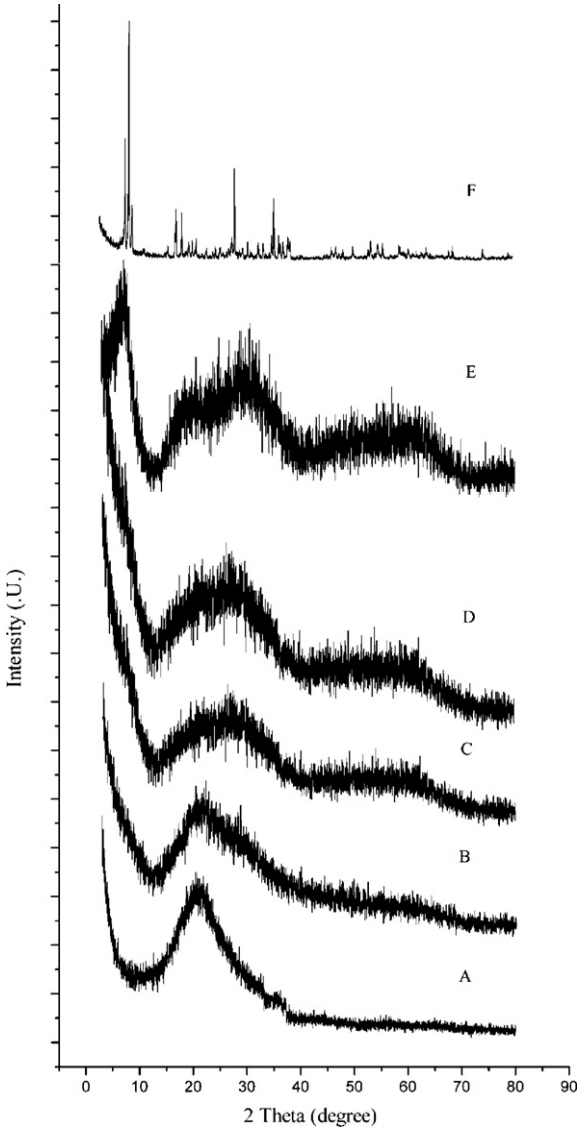

Fig. 4. XRD patterns of PSC (A), PS-EDA-HPW (B), PS-DETA-HPW (C), PS-TETA-HPW (D), PS-(AST-HPW)$_n$ (E), HPW (F).

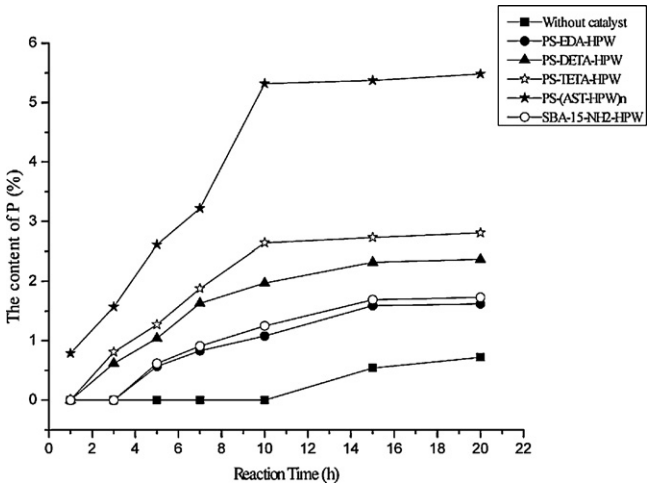

Fig. 5. Effect of reaction time on esterification reaction of POP1 using catalyst.

only 5.87 nm and POP1 was macromolecule with large dimension, it was difficult for POP1 to diffuse into the pore of SBA-15-NH_2-HPW, which decreased the efficiency of SBA-15-NH_2-HPW.

3.1.6. PSC_{HPW} stability and reusability

Catalyst reuse was an important step because it reduced the cost of the process. In order to verify the reusability, PS-(AST-HPW)$_n$ was tested in 10 h and reused five times. The contents of P were 5.34%, 4.98%, 5.22%, 5.14% and 5.07%, respectively. The relative standard deviation (R.S.D.) was 2.67%. The results showed no loss in the activity even after five cycles due to the strong interaction between the amine group and HPW, which demonstrated good stability of the catalyst. This meant that catalytic activity and durability of catalyst were predominant.

3.2. Characterization of POP1-p

Mw and DS_p of POP1-p were also investigated (Table 2). Results showed that Mw of the phosphorylated derivatives increased from 60.2 to 64.2 kDa, and DS_p increased from 0.09 to 0.33. It implied that hydroxyl groups were substituted successfully by phosphate groups in the polysaccharide. Compared with POP1-p5, DS_p (from POP1-p1 to POP1-p4) increased significantly. Furthermore, the reaction could achieve dynamic equilibrium quickly after an addition of catalyst. The fact that molecular mass of polysaccharide decreased after phosphorylated modification had not been observed. On the contrary, the molecular mass of POP1-p increased a little.

The FT-IR spectra of the native POP1 and POP1-p were shown in Fig. 2. Compared with POP1, three new strong absorption peaks appeared at 1717 cm^{-1}, 1269 cm^{-1} and 793 cm^{-1} for POP1-p, assigned to the C=O stretching vibration, the P=O asymmetric stretching and C–O–P symmetric vibrations, respectively. These absorptions indicated that the phosphorylated modification in the samples had actually occurred.

The phosphorylated position of polysaccharide was usually determined by ^{13}C NMR spectra. The ^{13}C NMR spectra of the native POP1 and its derivative (POP1-p4) were shown in Fig. 6. Compared with the signals of POP1, it was found that the signals of POP1-p4 became more complicated in ^{13}C NMR spectra. If the carbon is attached to an electron-withdrawing phosphate group, it would shift to a lower field position. On the contrary, the carbon indirectly attached to phosphate group would shift to higher field position [43]. The new peak of POP1-p4 at 57.9 ppm represented the signals of C-6p; the peak at 70.4 ppm represented the signal of C-2p. The peak at 60.9 ppm was weakened, which indicated that C-6 had

Table 2
Characterization of POP1-p.

POP1-p[a]	Catalyst	RT[b] (h)	Mw (kDa)	P (%)	DS_p
POP1-p1	PS-(AST-HPW)$_n$	3	60.2	1.57	0.09
POP1-p2	PS-(AST-HPW)$_n$	5	60.7	2.61	0.15
POP1-p3	PS-(AST-HPW)$_n$	7	62.8	3.22	0.19
POP1-p4	PS-(AST-HPW)$_n$	10	64.2	5.32	0.33
POP1-p5	Without catalyst	15	55.4	0.54	0.03

[a] Phosphorylation of polysaccharide from *Portulaca oleracea* L.
[b] Reaction time.

been substituted by the phosphate group, whereas C-2 had been substituted partially. We believed that the C-6 position was more active than the C-2 position due to the steric hindrance. Furthermore, a new peak at 98.7 ppm was assigned to C-1′, which showed that C-2 had been substituted, and could influence the adjacent C-1 to split into two peaks. New peaks at 70–80 ppm meant that phosphorylation of other positions had occurred besides C-6 and C-2.

3.3. Antioxidant activity analysis

3.3.1. Scavenging activity of hydroxyl radical

The hydroxyl radical, known to be generated through the Fenton reaction in this system, was scavenged by polysaccharide samples. The scavenging effects of all samples were shown in Fig. 7(A). For all the samples, the effects of scavenging hydroxyl radicals were in a concentration-dependent manner. POP1-p4 showed the best scavenging ability, and the scavenging ability was 44.3% at the concentration of 5.0 mg/mL, while the original POP1 showed a very low scavenging effect. The result indicated that the phosphate group played an important role in the scavenging of hydroxyl radicals.

For hydroxyl radical, one type of antioxidation mechanisms was reported that the scavenging activity of hydroxyl radical was due to the inhibition of hydroxyl radical generation by chelating ions such as Fe^{2+} [4]. Hydroxyl radicals could be generated by the reaction of Fe^{2+} and H_2O_2 ($Fe^{2+} + H_2O_2 \rightarrow Fe^{3+} + {}^{\bullet}OH + OH^-$), and since the phosphate group had chelating ability for Fe^{2+}, POP1-p could reduce the generation of hydroxyl radicals by chelating the Fe^{2+}.

3.3.2. Scavenging activity of superoxide radical

The superoxide radical (${}^{\bullet}O_2^-$) was a highly toxic species that was generated in a PMS/NADH system for being assayed in the reduction of NBT. Fig. 7(B) showed that the inhibitory effect of all different phosphorylated content samples on superoxide radical significantly increased with increasing concentration. At a concentration of 0.5 mg/mL, the scavenging effect was 63.8% and 75.2% for POP1-p3 and POP1-p4, respectively, but POP1-p5 and POP1 exhibited much weaker scavenging effect on superoxide radical.

In the study, antioxidation mechanism was that presence of phosphate groups could change the three-dimensional structure of polysaccharide, and increasing hydroxyl groups would emerge, which affected the antioxidant ability. Although superoxide was a relatively weak oxidant, it decomposed to form stronger and reactive oxidative species, such as singlet oxygen and hydroxyl radicals, which initiated peroxidation of lipids. Furthermore, superoxide was also known to indirectly initiate lipid peroxidation as a result of H_2O_2 formation, creating precursors of hydroxyl radicals [44]. The results indicated that the antioxidant activities of all the samples were related to their abilities to scavenge superoxide.

3.3.3. Scavenging activity of DPPH radicals

The model of scavenging the stable DPPH radical was a widely used method to evaluate antioxidant activities in a relatively short time compared with other methods (Fig. 7(C)). Both POP1-p3 and POP1-p4 had strong antioxidant activity, the scavenging effects were 66.9% and 51.4% at a dose of 5 mg/mL, higher than native POP1 but lower than BHA. However, the scavenging effects were 24.1% for POP1-p5 at the concentration of 5 mg/mL, which was weaker than that of POP1.

The effect of antioxidants on DPPH radical scavenging was possibly due to their hydrogen-donating abilities. DPPH$^{\bullet}$ was a stable free radical and could become a stable diamagnetic molecule when accepted an electron or hydrogen radical. In the present study, the phosphorylated derivatives showed excellent scavenging activity on DPPH radicals, which might be attributable to its strong hydrogen-donating ability compared to POP1.

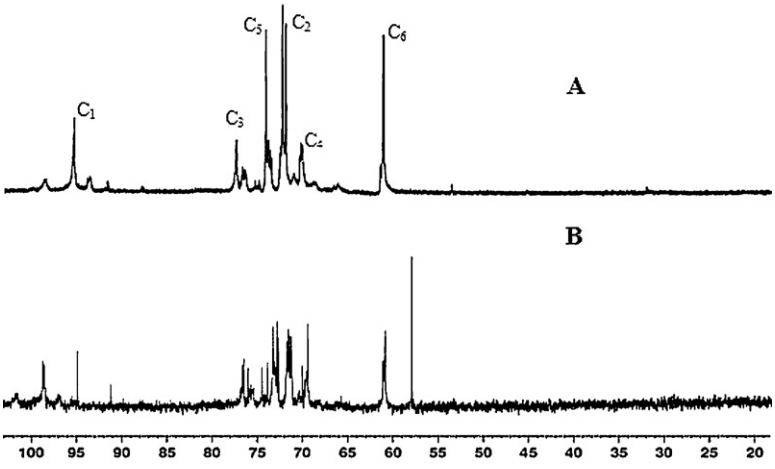

Fig. 6. ^{13}C NMR (600 MHz) spectra: (A) POP1; (B) POP1-p4.

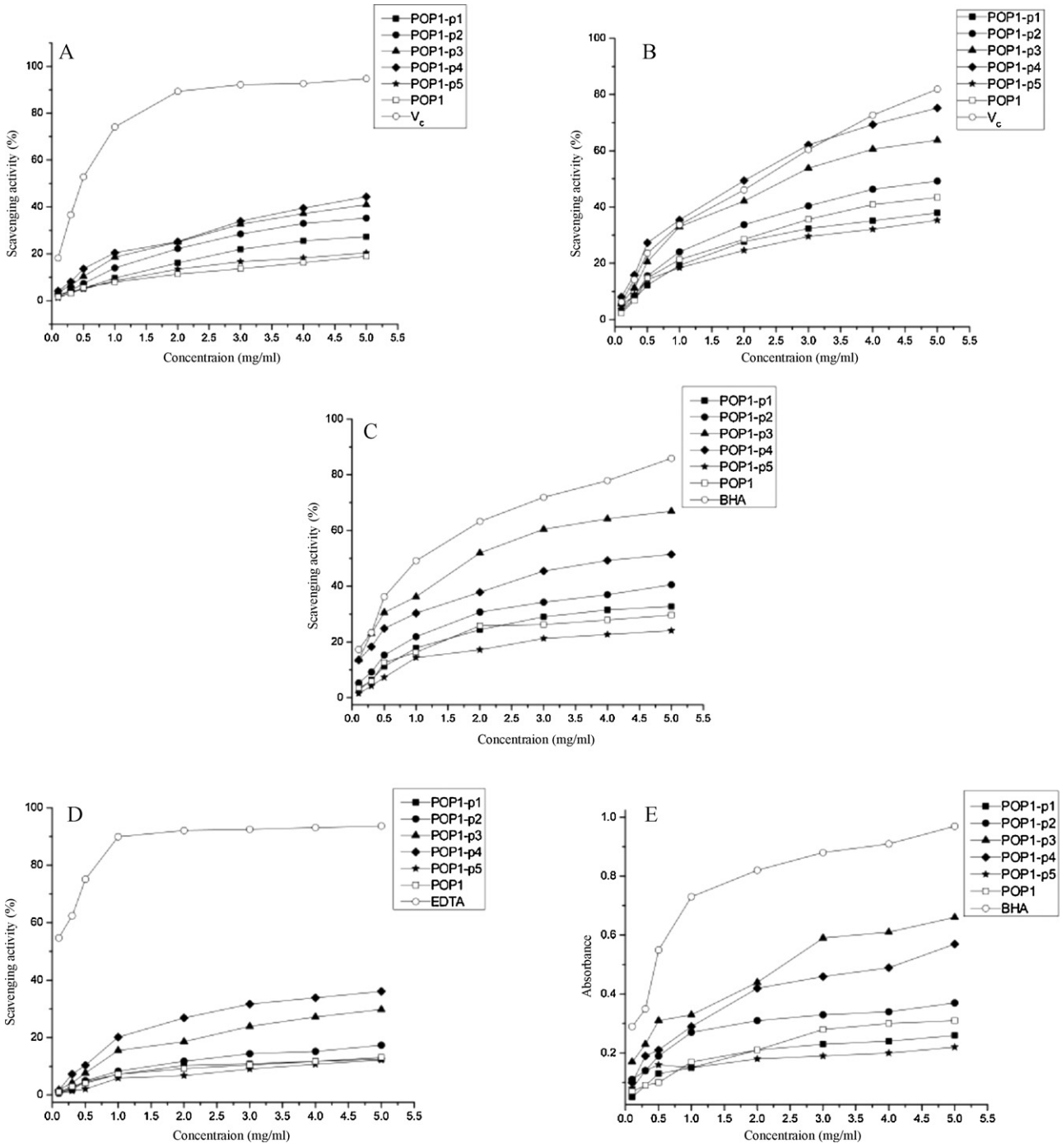

Fig. 7. Antioxidant effect of POP1 and POP1-p: (A) scavenging activity of hydroxyl radicals; (B) scavenging activity of superoxide radicals; (C) scavenging activity of DPPH radicals; (D) chelating effect on ferrous ions; (E) reducing power.

3.3.4. Chelating effect on ferrous ions

The ferrous ion chelating effects of POP1-p3 and POP1-p4 were concentration related and those of POP1-p1, POP1-p2 and POP1-p5 were not concentration dependent as shown in Fig. 7(D). Relationship between chelating effect and DS_p was obvious. At the concentration of 5 mg/mL, POP1-p3 and POP1-p4 showed the highest chelating abilities of 29.8% and 36.1%, respectively, but much lower than that of EDTA. Compared with the results, the phosphorylated derivatives showed moderate chelating ability on ferrous ions.

The antioxidant mechanism might be due to the supply of hydrogen by POP1-p, which combined with radicals and formed a stable radical to terminate the radical chain reaction. The other possibility was that POP1-p could combine with the radical ions which were necessary for radical chain reaction and then the reaction was terminated.

3.3.5. Reducing power

The reducing power of all samples was shown in Fig. 7(E). Both POP1-p3 and POP1-p4 had strengthen the reducing power, which were 0.66 and 0.57 at the concentration of 5 mg/mL, respectively, higher than that of native POP1 but lower than that of BHA. In contrast, the reducing power of POP1-p1 and POP1-p5 was only 0.26 and 0.22 at the concentration of 5 mg/mL, respectively. Compared with the results, the phosphorylated derivatives had

strong reducing capacity and the relation of reducing power to DS_p was significant.

The reducing properties were generally associated with the presence of reductone, which had been shown to exert antioxidant action through breaking the free radical chain by donating a hydrogen atom. Reductone was also reported to react with certain precursors of peroxide, thus preventing peroxide formation. In this assay, the phosphorylated derivatives with high donating-hydrogen ability showed excellent reducing power probably.

4. Conclusion

HPW was immobilized on PSC as an efficient stable solid acid catalyst for the phosphorylated modification of POP1. The high catalytic activity was attributed to the high surface area and Brönsted acid sites of the catalyst. Chemical equilibrium was established as quickly as 10 h with the content of P more than 5% using PS-(AST-HPW)$_n$. The catalysts could be removed from the medium by simple filtration and reused several times.

Four phosphorylated derivatives of POP1 from *P. oleracea* L. with different DS_p were synthesized using PS-(AST-HPW)$_n$ as catalyst. The structure and corresponding antioxidant activities were evaluated *in vitro*. Compared with native POP1, phosphorylated derivatives of POP1 showed greater antioxidant activities, which were affected by different DS_p. It could be expected that the phosphorylated derivatives of POP1 would have an assistant role as an antioxidant in the further.

References

[1] W.T. Xu, F.F. Zhang, Y.B. Luo, L.Y. Ma, X.H. Kou, K.L. Huang, Carbohyd. Res. 344 (2009) 217–222.
[2] E. Cadenas, K.J.A. Davies, Free Radic. Biol. Med. 29 (2000) 222–230.
[3] K. Uchida, Free Radic. Biol. Med. 28 (2000) 1685–1696.
[4] C. Zou, Y.M. Du, Y. Li, J.H. Yang, T. Feng, L. Zhang, Carbohyd. Polym. 73 (2008) 322–331.
[5] P. Ruperez, O. Ahrazem, J.A. Leal, J. Agric. Food Chem. 50 (2002) 840–845.
[6] S. Nandita, P.S. Rajini, Food Chem. 85 (2004) 611–616.
[7] H.M. Qi, Q.B. Zhang, T.T. Zhao, R. Chen, H. Zhang, X.Z. Niu, Z. Li, Int. J. Biol. Macromol. 37 (2005) 195–199.
[8] Y. Lu, D.Y. Wang, Y.L. Hu, X.Y. Huang, J.M. Wang, Carbohyd. Polym. 71 (2008) 180–186.
[9] Z.S. Zhang, Q.B. Zhang, J. Wang, X.L. Shi, H.F. Song, J.J. Zhang, Carbohyd. Polym. 78 (2009) 449–453.
[10] Z.M. Wang, L. Li, K.J. Xiao, J.Y. Wu, Bioresour. Technol. 100 (2009) 1687–1690.
[11] J. Wang, Q.B. Zhang, Z.S. Zhang, J.J. Zhang, P.C. Li, Int. J. Biol. Macromol. 44 (2009) 170–174.
[12] K.S. Parvathy, N.S. Susheelamma, R.N. Tharanathan, A.K. Gaonkar, Carbohyd. Polym. 62 (2005) 137–141.
[13] P.G. Dulce, B.C. Véronique, V. Rouet, M.E. Kerros, C. Klochendler, M.C. Tournaire, D. Barritault, J.P. Caruelle, E. Petit, Macromolecules 38 (2005) 4647–4654.
[14] X.Y. Che, X.J. Xu, L.N. Zhang, F.B. Zeng, Carbohyd. Polym. 78 (2009) 581–587.
[15] N. Garti, Y. Slavin, A. Aserin, Food Hydrocolloid 13 (1999) 145–155.
[16] N. Garti, A. Aserin, Y. Slavin, Food Hydrocolloid 13 (1999) 139–144.
[17] Y.F. Duan, G.P. Han, Chin. Food Chem. 26 (2005) 225–228.
[18] M.N. Timofeeva, M.M. Matrosova, T.V. Reshetenko, L.B. Avdeeva, A.A. Budneva, A.B. Ayupov, E.A. Paukshtis, A.L. Chuvilin, A.V. Volodin, V.A. Likholobov, J. Mol. Catal. A-Chem. 211 (2004) 131–137.
[19] D.P. Sawant, A. Vinu, J. Justus, P. Srinivasu, S.B. Halligudi, J. Mol. Catal. A-Chem. 276 (2007) 150–157.
[20] T.A. Peters, N.E. Benes, A. Holmen, J.T.F. Keurentjes, Appl. Catal. A-Gen. 297 (2006) 182–188.
[21] F. Collignon, R. Loenders, J.A. Martens, P.A. Jacobs, G. Poncelet, J. Catal. 182 (1999) 302–312.
[22] D.E. Lopez, J.G. Goodwin, D.A. Bruce, E. Lotero, Appl. Catal. A-Gen. 295 (2005) 97–105.
[23] A. Philippou, M.W. Anderson, J. Catal. 189 (2000) 395–400.
[24] W.Y. Lou, M.H. Zong, Z.Q. Duan, Bioresour. Technol. 99 (2008) 8752–8758.
[25] M. Hara, T. Yoshida, A. Takagaki, T. Takata, J.N. Kondo, S. Hayashi, K. Domen, Angew. Chem. Int. Ed. 43 (2004) 2955–2958.
[26] A. Alsalme, E.F. Kozhevnikova, I.V. Kozhevnikov, Appl. Catal. A-Gen. 349 (2008) 170–176.
[27] T. Blasco, A. Corma, A. Martınez, P. Martınez-Escolano, J. Catal. 177 (1998) 306–313.
[28] J.H. Sepulveda, J.C. Yori, C.R. Vera, Appl. Catal. A-Gen. 288 (2005) 18–24.
[29] M.E. Chimienti, L.R. Pizzio, C.V. Caceres, M.N. Blanco, Appl. Catal. A-Gen. 208 (2001) 7–19.
[30] Q.Y. Liu, W.L. Wu, J. Wang, Y.R. Wang, X.Q. Ren, Micropor. Mesopor. Mater. 76 (2004) 51–60.
[31] L.C. Passoni, F.J. Luna, M. Wallau, R. Buffon, U. Schuchardt, J. Mol. Catal. A-Chem. 134 (1998) 229–235.
[32] M.M. Heravi, F. Derikvand, F.F. Bamoharram, J. Mol. Catal. A-Chem. 263 (2007) 112–114.
[33] V.D. Vimary, Z.P. Tolstyka, H.D. Maynard, Macromolecules 42 (2009) 7650–7656.
[34] H. Liu, N.H. Xue, L.M. Peng, X.F. Guo, W.P. Ding, Y. Chen, Catal. Commun. 10 (2009) 1734–1737.
[35] Y.H. Tseng, J.H. Yang, J.L. Mau, Food Chem. 107 (2008) 732–738.
[36] X.Q. Zha, J.H. Wang, X.F. Yang, H. Liang, L.L. Zhao, S.H. Bao, J.P. Luo, Y.Y. Xu, B.B. Zhou, Carbohyd. Polym. 78 (2009) 570–575.
[37] M. Nishimiki, N.A. Rao, K. Yagi, Biochem. Biophys. Res. Commun. 46 (1972) 849–853.
[38] K. Shimada, K. Fujikawa, K. Yahara, T. Nakamura, J. Agric. Food Chem. 40 (6) (1992) 945–948.
[39] A. Braca, N.D. Tommasi, B.L.D. Di, C. Politi, L. Morelli, J. Nat. Prod. 64 (2001) 892–895.
[40] J.F. Yuan, Z.Q. Zhang, Z.C. Fan, J.X. Yang, Carbohyd. Polym. 74 (4) (2008) 822–827.
[41] G.D. Yadav, N. Kirthivasan, Appl. Catal. A-Gen. 154 (1997) 29–53.
[42] Y.X. Liu, W.W. Dai, T. Wang, Y. Tao, J. Chin. Central South Univ. Technol. 13 (2006) 451–455.
[43] A. Gamazade, S. Sklyar, I. Nasibov, A. Sushkov, Y. Shashkov, Y. Knirel, Carbohyd. Polym. 34 (1997) 113–116.
[44] M.K. Dahl, T. Richardson, J. Dairy Sci. 61 (1978) 400–407.